Further Characterization of the *psbH* Locus of *Synechocystis* sp. PCC 6803: Inactivation of *psbH* Impairs Q_A to Q_B Electron Transport in Photosystem 2†

Steve R. Mayes,‡,∥ James M. Dubbs,‡ Imre Vass,§ Éva Hideg,§ Laszlo Nagy,‡ and James Barber*,‡

AFRC Photosynthesis Research Group, Wolfson Laboratories, Biochemistry Department, Imperial College of Science, Technology and Medicine, London, U.K., and Biological Research Centre, H-6701 P.O. Box 521, Szeged, Hungary

Received July 13, 1992; Revised Manuscript Received November 23, 1992

ABSTRACT: The *psbH* gene encodes a small protein which copurifies with photosystem 2. In the cyanobacterium *Synechocystis* sp. PCC 6803, *psbH* is located upstream of the cytochrome b_6–*f* complex genes *petC* and *petA*. In striking contrast, in the genomes of plant chloroplasts, *psbH* is cotranscribed with *petB* and *petD*, encoding the other two major subunits of the cytochrome b_6–*f* complex. We report that in *Synechocystis* sp. PCC 6803 monocistronic *psbH* and dicistronic *petCA* transcripts are probably initiated separately, each from DNA regions bearing some similarity to *Escherichia coli* σ^{70} promoters. *Synechocystis* sp. PCC 6803 *psbH* null mutants were generated by cartridge mutagenesis. Studies using a rapid screening procedure involving in situ complementation showed that the PsbH protein is not absolutely required for the assembly of a functionally active photosystem 2 complex since *psbH* insertion and deletion strains were able to grow photoautotrophically. The rate of photoautotrophic growth was, however, slower than the wild type, and studies of oxygen evolution, chlorophyll fluorescence, and thermoluminescence indicated that this reduction in growth rate is probably due mainly to an impairment in electron flow from Q_A to Q_B. We conclude, therefore, that the PsbH protein is not an absolute requirement for photosystem 2 activity but that it functions to optimize electron flow between the two secondary plastoquinone acceptors by interacting with the Q_B site on the D1 protein.

Many important membrane complexes consist of proteins that are additional to those subunits that carry the catalytic center. This is particularly true for complexes involved in respiratory and photosynthetic electron transfer and energy conversion. Presumably, many of these "attendant" proteins are needed for optimization and regulation of the particular functional activity. One such protein is the product of the *psbH* gene which is a noncatalytic subunit of the photosystem 2 (PS2)[1] complex of oxygenic photosynthesis [reviewed in Andersson and Styring (1991)].

The *psbH* gene product was first detected in pea chloroplasts as a 9-kDa phosphoprotein (Bennett, 1977). The phosphorylation reaction is reversible and seems to be controlled by the redox state of the plastoquinone pool in a manner similar to that observed with the PS2 light-harvesting chlorophyll *a*/*b* complex [Allen et al., 1981; see also Knaff (1991)]. Although the precise function of the PsbH protein has remained elusive, it has been speculated that it plays a role in regulating and stabilizing secondary electron transfer at the level of the two plastoquinone acceptors, Q_A and Q_B (Hodges et al., 1985; Packham et al., 1988). Other studies have implicated the PsbH protein in the process of photoinhibition (Kuhn et al., 1988).

To elucidate the role of the PsbH protein, the approach we have adopted here is to examine the phenotypic consequences of inactivating the *psbH* gene in vivo. As it is difficult to target specific gene interruptions or deletions into either the nuclear or the chloroplast genomes of plants, we are using the cyanobacterium *Synechocystis* sp. PCC 6803 (hereafter called *Synechocystis* 6803) to study the influence of different PS2 genes. The PS2 of *Synechocystis* 6803 is similar to that of plants, yet the organism is readily transformed by exogenous DNA and is capable of growing photoheterotrophically when PS2 activity is impaired [see Williams (1988)].

As a prelude to targeted mutagenesis of *psbH*, we recently sequenced the *Synechocystis* 6803 *psbN–psbH–petC–petA* gene cluster (Mayes & Barber, 1991). The *petC* and *petA* genes respectively encode the Rieske Fe–S protein and apocytochrome *f* subunits of the cytochrome b_6–*f* complex. In striking contrast, the *psbH* gene of plant chloroplast genomes is cotranscribed with *psbB*, *petB*, and *petD* encoding, respectively, the PS2 chlorophyll *a*-binding protein CP47 and the other major cytochrome b_6–*f* complex subunits, apocytochrome b_6 and subunit IV (Hird et al., 1986; Westhoff et al., 1986). The *psbN* gene, which encodes another low molecular mass protein associated with PS2 (Ikeuchi et al., 1989), is located upstream of *psbH* on the opposite DNA strand in both plant chloroplasts and *Synechocystis* 6803. Interestingly, sequence analysis also reveals that the *Synechocystis* 6803 PsbH protein is truncated at the amino terminus compared with chloroplast sequences and thus lacks the conserved chloroplast protein phosphorylation site (Abdel-Mawgood & Dilley, 1990; Mayes & Barber, 1990).

In this paper, we have first further characterized the *psbH* locus of *Synechocystis* 6803, paying particular attention to transcription of *psbH*, *petC*, and *petA*. With this knowledge, a number of mutant strains not able to synthesize the PsbH protein were constructed. One of these mutants was then selected for more detailed biophysical characterization to establish the nature of the lesion in PS2 that it harbors.

† This work was supported by the Agricultural and Food Research Council, the Science and Engineering Research Council, and the Hungarian Academy of Sciences (OTKA 888) and UNIDO–ICGEB (CRP/GRE 90-01). L.N. was the recipient of a Royal Society and Hungarian Academy of Science Fellowship.

* Author to whom correspondence should be addressed.

‡ Imperial College of Science, Technology and Medicine.

∥ Present address: Stratagene Ltd., Cambridge, U.K.

§ Biological Research Centre, Szeged.

[1] Abbreviations: DMQ, dimethyl-*p*-benzoquinone; FeCy, potassium ferricyanide; DCBQ, dichloro-*p*-benzoquinone; PS1, photosystem 1; PS2, photosystem 2; DCMU, 3-(3,4-dichlorophenyl)-1,1-dimethylurea.

0006-2960/93/0432-1454$04.00/0

MATERIALS AND METHODS

Strain and Culture Conditions. The materials used were described in Mayes et al. (1991). The *Synechocystis* sp. PCC 6803 strain studied was the glucose-tolerant strain *Synechocystis* 6803-G (Williams, 1988), referred to throughout as the wild-type strain. This was kindly provided by Dr. J. G. K. Williams (DuPont, Wilmington DE). Routine wild-type and mutant growth and manipulation were as described in Mayes et al. (1991). For ease of discussion, the three growth conditions used throughout are defined according to Astier et al. (1984) as photoautotrophic (light, BG-11), photoheterotrophic (light, BG-11, 5 mM glucose, 20 μM atrazine), and mixotrophic (light, BG-11, 5 mM glucose) where BG-11 is the culture medium described in Williams (1988). Plates supporting photoautotrophic, photoheterotrophic, or mixotrophic growth are referred to in the text as PA, PH, or M plates, respectively. Growing photoautotrophically, *Synechocystis* 6803 requires PS2 to participate in linear photosynthetic electron transport from which the NADPH and ATP, necessary for CO_2 fixation, are generated. In photoheterotrophic growth, with PS2 inactivated, it has been assumed that light drives cyclic photophosphorylation (Rippka, 1972; Astier et al., 1984; Williams, 1988). Recently, light-activated heterotrophic growth (LAHG) of *Synechocystis* 6803 has been characterized (Anderson & McIntosh, 1991). These authors reported that the LAHG rate is slower than the photoheterotrophic growth rate, which is in keeping with the apparent trend that for cyanobacteria chemotrophy (where possible) promotes slower growth than photoheterotrophy (Smith, 1982). This difference is consistent with the current view that cyclic photophosphorylation provides a significant energetic contribution during photoheterotrophic growth of *Synechocystis* 6803. In our experiments, *Synechocystis* 6803 was grown in continuous white light at 32 °C. For the in situ complementation experiments, plates were incubated in a Fison growth cabinet (Model 60063TTL), and the light intensity was measured with a Li-cor LI-185 quantum photometer. Liquid cultures for biophysical characterization were grown mixotrophically with continuous orbital shaking in conical flasks; 100 μg mL^{-1} kanamycin was added to IC7 cultures to maintain selection.

DNA Isolation, Manipulation, and Southern Analysis. General DNA manipulations, including maxiprep isolation of wild-type *Synechocystis* 6803 DNA, radiolabeling of double-stranded DNA probes, and Southern analysis, were as described in Mayes et al. (1991). Plasmids were isolated from the *dam Escherichia coli* strain JM110 (Yanisch-Perron et al., 1985) when restriction with *Bcl*I was required. The high-stringency Southern conditions used in Figure 6 consisted of hybridization overnight at 65 °C in 10 mL of 5 × SSC, 5 × Denhardt's, 0.5% SDS, and 100 μg mL^{-1} denatured sonicated calf thymus DNA with filter washing to a final stringency of 0.1 × SSC/0.1% × SDS at 65 °C [solutions defined in Mayes et al. (1991)]. Mutant strain DNAs used in this analysis were prepared according to the chromosomal DNA miniprep method previously reported (Mayes et al., 1991).

Northern Analysis of Synechocystis 6803 Transcripts. RNA from late-exponential-phase cultures grown mixotrophically was extracted and subjected to Northern analysis as in Mayes et al. (1991). M13 mp18 and mp19 (Yanishch-Perron et al., 1985) clones generated by directional subcloning for sequencing the gene cluster (Mayes & Barber, 1991) were used as templates to generate high specific activity single-stranded DNA probes, essentially as described in Mayes et al. (1991). Following radiolabel incorporation, the reaction products were incubated with suitable restriction enzymes to ensure that all M13 sequences would be removed at the denaturing gel electrophoresis stage.

Transcript Mapping by Primer Extension. Primer extension mapping of the 5′ end points of mRNAs was performed by the method of Ausubel et al. (1987), using avian myoblastosis virus reverse transcriptase (Boehringer Mannheim Biochemicals) and the aqueous hybridization option recommended for oligonucleotide primers. Total *Synechocystis* 6803 RNA, isolated as for the Northern analysis, was used in the extension reaction. Extension products were sized by electrophoresis on a urea sequencing gel alongside a ^{35}S-sequencing ladder. This DNA sequencing was performed using the dideoxy chain termination method on denatured plasmid subclone templates as described by Cantrell and Bryant (1987). Plasmid templates were purified by CsCl/ethidium bromide centrifugation (Maniatis et al., 1982).

Mutant Strain Construction. Mutant strains were engineered by transforming the following plasmid constructs into *Synechocystis* 6803: plasmid pSMH21 for generating strain IC3; pSMH22 for IC4; pSMH23 for IC5; pSMH24 for IC6; pSMH25 for IC7; pSSH3 for IC8. These constructs were introduced and the homozygous mutants segregated as described in Mayes et al. (1991). Briefly, the constructs were made as follows. pSMH21: The pUC4K kanamycin resistance cartridge [variant described in Taylor and Rose (1988) and referred to throughout as Km^r] excised by *Eco*RI was ligated into the *Eco*RI site upstream of *psbH* in pSMH8 (described in Figure 7) to generate pSMH21. pSMH22: The purified *Eco*RI–*Hin*dIII insert of plasmid pSMH10 (described in Figure 1B) was restricted with *Hpa*II. The resulting fragments were ligated simultaneously with the *Acc*I-delimited Km^r, and plasmid pUC18 (Yanisch-Perron et al., 1985) was linearized by *Eco*RI and *Hin*dIII. Construct pSMH22 was subsequently selected by restriction mapping transformant plasmids. pSMH23: The 1.6-kb *Synechocystis* 6803 *Hin*dIII–*Xba*I fragment containing *psbN* and *psbH* was subcloned into pUC18 to form plasmid pSMH11. Plasmid pSMH23 was then generated by restricting pSMH11 with *Hin*cII, purifying the large fragment, and then ligating into this the *Hin*cII-delimited Km^r. pSMH24, pSMH25: The 1.2-kb *Synechocystis* 6803 *Ssp*I–*Eco*RI fragment containing *psbN* and *psbH* was ligated into pUC19 (Yanisch-Perron et al., 1985) linearized by *Hin*cII and *Eco*RI, to form pSMH12. Plasmid pSMH24 was then made by ligating the *Hin*cII-delimited Km^r into the *Eco*RV site of pSMH12. The same Km^r was ligated into the purified large *Eco*RV–*Hin*cII fragment of pSMH12 to generate pSMH25. pSSH3: The 4.2-kb *Hin*dIII–*Hin*dIII insert of pSMH8 was transferred to pUC9 (Vieira & Messing, 1982) to generate pSSH1. Construct pSSH3 was then made by replacing the 0.9-kb *Eco*RI–*Xba*I fragment in pSSH1 containing *psbN* and *psbH* with the *Eco*RI–*Xba*I-delimited Km^r from pSSKm1 [described in Mayes et al. (1991)].

In Situ Genetic Complementation. This method was adapted from the experiments of Dzelzkalns and Bogorad (1988), and the procedure used here was as in Mayes et al. (1991). For M and PH plates, final concentrations of 5 mM glucose and 5 mM glucose plus 20 μM atrazine, respectively, in addition to their inclusion in the base agar, were also mixed with the top agar immediately prior to pouring the overlay.

Fluorescence Measurements. Chlorophyll fluorescence measurements were conducted on cells that had previously been given 50 preflashes of bright white light and incubated in the dark at room temperature for 10 min. Such pretreatment

standardizes the redox status of the electron-transport components and, in particular, oxidizes the plastoquinone pool. Induction kinetics were obtained using a pulse amplitude modulated fluorimeter (PAM 101, Walz). Actinic light was provided by an Intralux (150 W) light source fitted with a Uni-blitz electronic shutter. The light beam was filtered using RG630 red filters to an intensity of 80 μE m^{-2} s^{-1}. Readings were obtained using 30 μg of Chl *a* (mL of cell suspension)$^{-1}$. For some measurements, the cells were treated with 40 μM DCMU [3-(3,4-dichlorophenyl)-1,1-dimethylurea, an electron-transport inhibitor] for 2 min before induction commenced; alternatively, hydroxylamine plus DCMU treatment was as described by Philbrick et al. (1991). To measure the fluorescence decay, 1.5 mL of harvested and resuspended cells (30 μg of Chl *a* mL^{-1}) was deposited onto a Millipore membrane filter. Fifty preflashes were applied, and after 10-min dark-adaptation, measurements were taken. The distance between the sample surface and the end of the fiber optic was approximately 1 mm. The single actinic flash having approximately 10 000 μE m^{-2} s^{-1} intensity was given by the attached XST 103 xenon flash lamp unit. The frequency of the measuring beam was 100 kHz and data points were collected every 25 μs using the Walz A/D converter and DA100 software.

Thermoluminescence Measurements. Thermoluminescence was measured with a home-built apparatus as previously described (Vass et al., 1981) at 50 μg of Chl *a* mL^{-1}. Before thermoluminescence measurements were conducted the cells were preilluminated with white light of 50 μE m^{-2} s^{-1} intensity for 30 s, followed by a 5-min dark-adaptation period at room temperature. As previously described (Vass et al., 1992), this pretreatment ensures reproducible dark distribution of S-states. Thermoluminescence was excited at 5 °C by a series of single-turnover flashes (3 μs) provided by a General Radio Stroboslave 1539-A xenon flash at 1-Hz frequency. Following flash excitation, the samples were quickly cooled down in the dark to –40 °C, from where the slow heating with a rate of 20 °C min^{-1} was initiated, and thermoluminescence was detected; 40 μM DCMU was added, when indicated, after 30-s preillumination in continuous light at the beginning of the 5-min dark-adaptation period.

Steady-State Oxygen Evolution Measurements. Steady-state, light-saturated rates of oxygen evolution were measured at 31 °C using a Hansatech DW2 O_2 electrode at a light intensity of 3000 μE m^{-2} s^{-1}. The measurements were performed in fresh BG-11, either without artificial electron acceptors or in the presence of 1 mM dimethyl-*p*-benzoquinone, with or without 1 mM potassium ferricyanide or 1 mM dichloro-*p*-benzoquinone.

Flash Oxygen Measurements. The flash dependence of oxygen evolution was measured with an unmodulated bare-platinum oxygen electrode as described earlier (Vass et al., 1990). Cell suspensions were used at 50 μg of Chl *a* mL-$^{-1}$ without artificial electron acceptors, and were preilluminated with a train of 50 flashes followed by 5-min dark-adaptation. Oxygen evolution was induced by a series of short (3 μs) flashes provided by a General Radio Stroboslave 1539-A xenon flash at 1-Hz frequency. Signals were detected by a home-built amplifier. Data acquisition was controlled by an IBM XT compatible computer equipped with an analogue/digital converter card (14 bit, 25 μs).

RESULTS

Analysis of the psbN–psbH–petC–petA Gene Cluster. We have previously reported the isolation of λEMBL3 library clones containing the *psbH* gene of *Synechocystis* 6803 (Mayes et al., 1990). Three of these clones were subjected to Southern analysis, and the restriction map shown in Figure 1A of about 25.1 kb of the *Synechocystis* 6803 chromosome surrounding the gene cluster was generated. Figure 1B shows a more detailed map of the 4.2-kb *Hin*dIII–*Hin*dIII fragment containing the cluster.

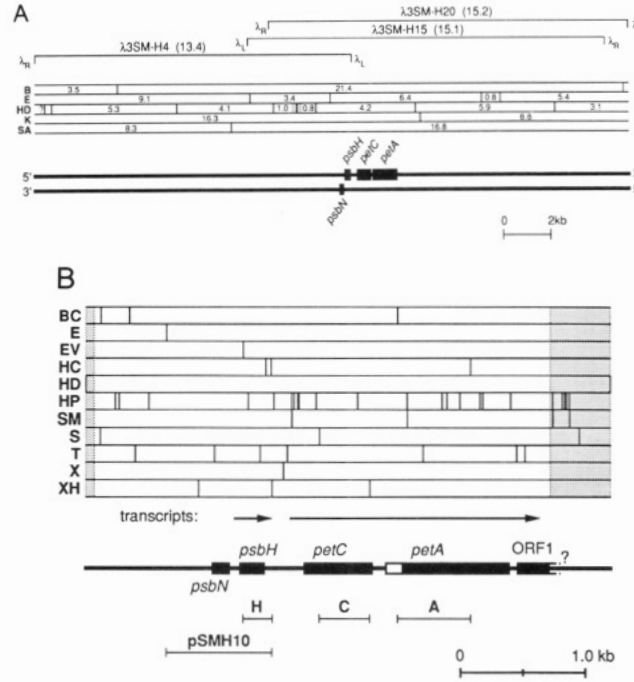

FIGURE 1: Organization of the *psbN–psbH–petC–petA* gene cluster in *Synechocystis* 6803. The restriction sites shown are as follows: B, *Bam*HI; BC, *Bcl*I; E, *Eco*RI; EV, *Eco*RV; HC, *Hin*cII; HD, *Hin*dIII; HP, *Hpa*II; K, *Kpn*I; SM, *Sma*I; SA, *Sal*I; S, *Ssp*I; T, *Taq*I; X, *Xba*I; XH, *Xho*II. (A) Restriction map of about 25.1 kb of the *Synechocystis* 6803 genome that is contained in three overlapping library phage clones, λ3SM-H4, λ3SM-H15, and λ3SM-H20. These clones resulted from the ligation of chromosomal DNA partially restricted with *Sau*3A into the *Bam*HI site of λEMBL3 [see Mayes et al. (1990)]. The λEMBL3 vector left and right arms are denoted by λ_R and λ_L, respectively, and the numbers estimate restriction fragment sizes (kb). ? marks an uncertain site while the stippled *Hin*dIII site denotes that the linear order of the 1.0- and 0.8-kb *Hin*dIII fragments has not been deduced. (B) More detailed restriction map of the 4.2-kb *Hin*dIII–*Hin*dIII DNA fragment containing the gene cluster. The unshaded region of this map was generated from the DNA sequence (Mayes & Barber, 1991). The sites reported within the shaded regions were identified by a combination of restriction mapping and sequencing in one orientation only and may therefore not be complete. The extent of the *petA* presequence is shown as an open box. ORF1 is an open reading frame identified by sequencing (Mayes & Barber, 1991). It is not known how far ORF1 extends or if it is transcribed (see text). The pattern and extent of transcripts determined in this paper are arrowed. The *Eco*RI–*Xho*II restriction fragment that was subcloned into pBS+ (formerly Bluescribe M13+, Stratagene) to generate plasmid pSMH10 is indicated. Also labeled H, C, and A, respectively, are DNA regions that were subcloned into M13 to generate the strand-specific probes used in Figure 2.

Low-stringency Southern analysis (not shown) demonstrated that there are single copies of *petC* and *petA* in the *Synechocystis* 6803 genome, as we reported for *psbH* (Mayes & Barber, 1990). Experiments also suggested that *psbN* is single-copy, although owing to the small size of this gene (132 bp) this conclusion would best be verified in the future by attributing an altered phenotype to a specific *psbN* null mutant.

Transcription of the psbH, petC, and petA Genes. Steady-state chloroplast transcripts encompassing the entire *psbB* operon can be detected from a variety of plants [e.g., see

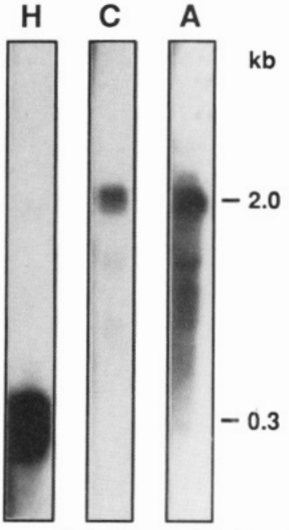

FIGURE 2: Northern analysis of transcripts from the *Synechocystis* 6803 *psbH*, *petC* and *petA* genes. ^{32}P-Labeled strand-specific probes were hybridized to Northern blots of total *Synechocystis* 6803 RNA (approximately 10 μg per lane). Probe H was a *psbH*-specific *Eco*RV–*Xho*II fragment; probe C was a *petC*-specific *Ssp*I–*Xho*II fragment; probe A was a *petA*-specific *Bcl*I–*Hin*cII fragment. The location of these DNA fragments is shown in Figure 1B.

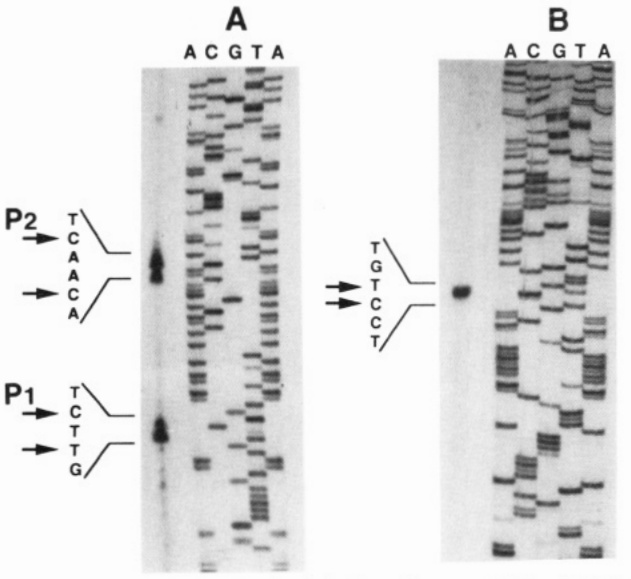

FIGURE 3: Mapping the 5′ ends of the *Synechocystis* 6803 *psbH* (A) and *petCA* transcripts (B) by primer extension. Panel A shows the extension products generated by using the *psbH*-specific oligonucleotide primer 5′-CCTTACCGTATTCCGAGTTG-3′. Panel B shows the result of using the *petCA*-specific primer 5′-CCAGAAATCTGTGTCAT-3′. In both experiments, the extension products are sized against a ^{35}S-sequencing ladder generated using the same oligonucleotide primer as was used in the extension reaction. The nucleotides at the 5′-transcript ends are arrowed, and the two end-point regions in panel A are marked P1 and P2. It should be noted that faint bands in the sequencing ladders shown here have previously been confirmed through sequencing of the opposite strand (Mayes & Barber, 1991).

Kohchi et al. (1988), Westhoff and Herrmann, (1988), and Westhoff et al. (1991)]. Therefore, prior to conducting mutagenesis, it was considered important to investigate whether a comparable *Synechocystis* 6803 transcript spanning *psbH*, *petC*, and *petA* could be detected. This was addressed by Northern blotting using single-stranded gene-specific probes as shown in Figure 2. The *psbH*-specific probe hybridized to a 0.3-kb mRNA. Since the *psbH* gene consists of 195 bp, this transcript is just large enough to encode the whole gene. Importantly, the *psbH* probe was not seen to hybridize to any higher molecular weight RNA species, even when the autoradiogram was overexposed (not shown). The *petC*-specific and *petA*-specific probes both hybridized to the same 1.9–2.0-kb mRNA, which interestingly is the same size as the *Nostoc* sp. PCC 7906 *petCA* transcript (Kallas et al., 1988).

Mapping the 5′ Ends of the psbH and petCA Transcripts in Synechocystis 6803. To map the 0.3-kb *psbH* and 2.0-kb *petCA* mRNAs, their 5′ ends were determined by primer extension. As shown in Figure 3, both transcripts yielded sharp defined signals rather than a series of end points. The sequence location of these end points is shown in Figure 4. It can be seen that the *psbH* transcript 5′ termini are located in two regions. The first, designated P1, consists of two end points at A and G residues in positions –40 and –42 relative to the *psbH* translation start, respectively. The second region, designated P2, consists of two end points at two G residues in positions –67 and –70. Immediately 5′ to the *psbH* P1 transcription start is the sequence element TATTAT which is similar to the "–10" region of the major vegetative σ^{70} promoter in *E. coli* [see Harley and Reynolds (1987) and Collado-Vides et al. (1991)]. Additionally, the sequence TTGATA, resembling an *E. coli*-like "–35" σ^{70} promoter element, occurs from positions –71 through –76. The spacing between these two elements of 18 bp compares well to the 16–18 bp most frequently observed between "–10" and "–35" elements in *E. coli* (Harley & Reynolds, 1987). In contrast, the *psbH* P2 transcription start is also immediately preceded by a sequence element (TAAGAT) possessing some similarity to the σ^{70} consensus "–10" region, but there is little similarity in the "–35" region.

As Figure 4B shows, the 5′ termini of the *petCA* mRNA map to two adjacent G residues at positions –129 and –130 relative to the candidate *petC* translation start which is conserved in the *Nostoc* sp. PCC 7906 sequence [discussed in Mayes et al. (1991)] and also that of *Synechococcus* sp. PCC 7002 (Widger, 1991). The sequence immediately upstream of the transcription starts contains the element TGTCATAAT which shows similarity to the *E. coli* σ^{70} "–10" consensus sequence in two different alignments (shown in Figure 4B). The nearest sequence resembling a "–35" element (TTGTCT) occurs 20 or 23 bp upstream from the candidate "–10" elements at positions –166 through –171. If the 2.0-kb size of the *petCA* transcript is accurate (Figure 2), then this places the 3′-transcript end approximately 180 bp within the downstream ORF1 (see Figure 1B). [As yet, we have no evidence that ORF1 is a coding region. The codon usage of the 5′ portion of this ORF does not correlate well with that of 34 characterized genes from *Synechocystis* 6803 (Mayes, 1992).]

Cartridge Mutagenesis of psbH. Cartridge mutagenesis was used to study the effect of inactivating the *psbH* gene. The mutant strains that were engineered are shown in Figure 5 (see Materials and Methods for construction details). An important element of the approach was to introduce control mutations upstream and downstream of *psbH* (strains IC3 and IC5) in regions predicted to be nonfunctional. The kanamycin resistance cartridge (Km^r) in IC5 is positioned 139 and 140 bp upstream of the mapped 5′ end points of *petCA* transcripts, which we argue (see Discussion) are transcription initiation points. Initially, strains IC3, IC4, and IC5 were generated. However, due to the photoautotrophic growth character of IC4, strains IC6, IC7, and IC8 were also constructed.

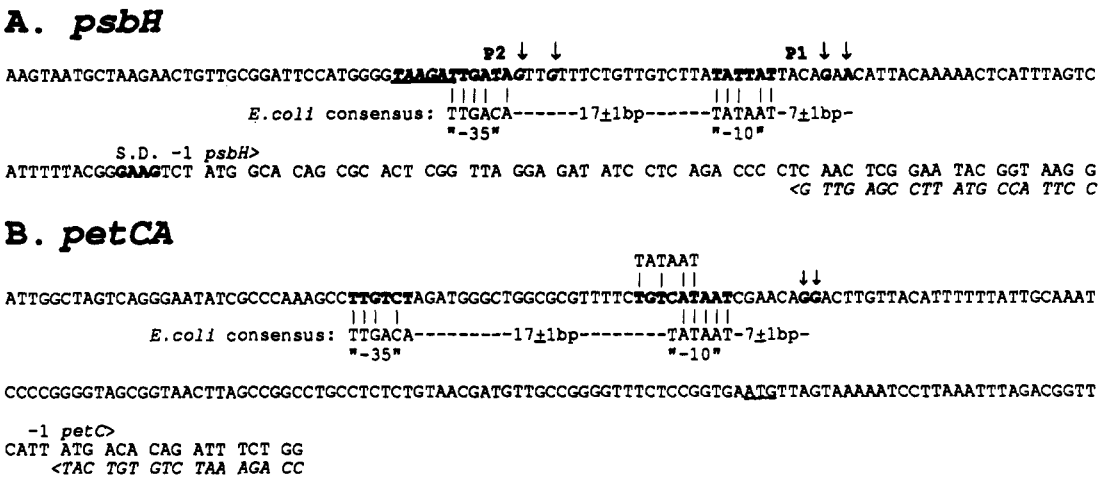

FIGURE 4: DNA sequence location of the 5′ end points of the *psbH* and *petCA* transcripts of *Synechocystis* 6803. (A) Sequence 5′ to the *psbH* translation start. The 5′ *psbH* transcript end points within the two regions P1 and P2 are arrowed, and the candidate ribosome binding site is denoted "S.D". Matches between sequence elements upstream of P1 and the *E. coli* σ^{70} promoter consensus defined by Harley and Reynolds (1987) are marked, and an element upstream of P2 with similarity to the "−10" σ^{70} region is italicized and underlined. Also shown is the oligonucleotide primer used in the mapping experiments (<). (B) Sequence 5′ to the candidate *petC* translation start which is conserved with *Nostoc* sp. PCC 7906 and *Synechococcus* sp. PCC 7002 (Widger, 1991). The other potential translation start is underlined [see Mayes and Barber (1991) for a discussion]. The 5′ end points of the *petCA* transcript are again arrowed, upstream sequence elements with similarity to the *E. coli* σ^{70} consensus are highlighted, and the positions of the oligonucleotide primer used for mapping are indicated (<).

As *Synechocystis* 6803 contains approximately 12 chromosomal copies per cell (LaBarre et al., 1989), it was necessary to verify that segregation of mutants homozygous for the introduced mutation had been achieved. After several rounds of restreaking transformants (see Materials and Methods), genomic DNA was isolated from each mutant and subjected to Southern analysis. Figure 6 shows typical results, following digestion with *Ssp*I. Similar experiments using other restriction enzymes were also performed (not shown). Figure 6 shows that no copies of the wild-type 1753 bp *Ssp*I–*Ssp*I fragment containing *psbH* were detected in any of the mutant strains IC3–IC8. Instead, the sizes of hybridizing *Ssp*I–*Ssp*I fragments correspond to those calculated for each mutant strain in Figure 5.

For a merodiploid state to persist in any one of the mutant strains, at least one wild-type *psbH* locus would have to be retained per *Synechocystis* 6803 cell. Consequently, in a merodiploid strain, at least 1 *psbH* locus in 11 would be wild type, a level that would have been readily detectable in Figure 6, if such a wild-type population had existed. Figure 6, and also the other genome Southern blots not shown, demonstrates that for each mutant strain, the introduced mutation has been substituted into every chromosomal copy per cell. Supporting this conclusion, comparable Southern experiments have successfully detected merodiploid *Synechocystis* 6803 strains in other mutagenesis studies. Such experiments revealed that our initial attempt to construct a *psbO* deletion strain by deleting 2.4 kb of the *Synechocystis* genome containing *psbO* resulted in merodiploid strains that would not segregate. Subsequently, we found that the 2.4-kb region contained an essential *trnQ* gene alongside *psbO* (Mayes, 1992). Similarly, Smart et al. (1991) readily characterized merodiploid strains by Southern analysis in mutagenesis experiments targeting the *psaA* gene of photosystem I.

In addition, the data from Figure 6 and the other Southern blots not shown verified the restriction maps shown in Figure 5 and in particular confirmed the orientation of the Km^r in each mutant strain.

Ability of the psbH Null Mutants To Grow Photoautotrophically. A preliminary investigation of PS2 activity in strains IC3, IC4, and IC5 was performed by streaking out each strain, and also the wild-type, on agar plates, permitting either photoautotrophic growth, where PS2 activity is essential, or photoheterotrophic growth, where PS2 is not required (PA and PH plates, respectively; see Materials and Methods). The plates were incubated at 32 °C, 50–60 μE m^{-2} s^{-1} illumination.

Both control strains, IC3 and IC5, grew well, in a manner indistinguishable from the wild-type on both PA and PH plates. In contrast, IC4 grew well on PH plates but less well on PA plates, where it exhibited a reluctance to form single colonies. This altered behavior of IC4 caused us to construct strains IC6, IC7, and IC8. It was found that these additional strains grew similarly on PA plates to IC4. Subsequent analysis showed that all the *psbH*-less strains grew better on PA plates when illuminated at a lower light intensity (5 μE m^{-2} s^{-1}).

In Situ Complementation Studies. Because of the abnormal growth of *psbH* null mutants on PA plates, the technique of in situ complementation was adapted to study the growth of strains on PA, PH, and M plates under reproducible conditions at 5 μE m^{-2} s^{-1} light intensity. This technique has been employed previously for selecting useful genomic library clones (Dzelzkalns & Bogorad, 1988) and for verifying a mutant genotype (Mayes et al., 1991). The method assays the viability and growth rate of strains growing on plates from single isolated cells. The wild-type gene is reintroduced into the mutant in one area of the plate by spotting DNA onto an agar overlay of mutant cells. A direct visual comparison between the growth rates of cells containing an inactivated or a functional target gene can be made at the transformation interface (TI).

Figure 7A shows the results of in situ complementation experiments using the wild-type control and IC7. Such experiments were repeated at least 3 times with all the mutant strains, IC3–IC8.

Control strains IC3 and IC5 yielded the same results as those for the wild-type (Figure 7A). None of these three strains were visibly complemented by plasmid pSMH8 containing *psbN*, *psbH*, *petC*, and *petA* or by pSMH10 containing just *psbN* and *psbH* (plasmid described in Figure 1B legend; results not shown). These results are consistent with the DNA sequence data (Mayes & Barber, 1991) which suggest the mutation sites in IC3 and IC5 are within noncoding DNA.

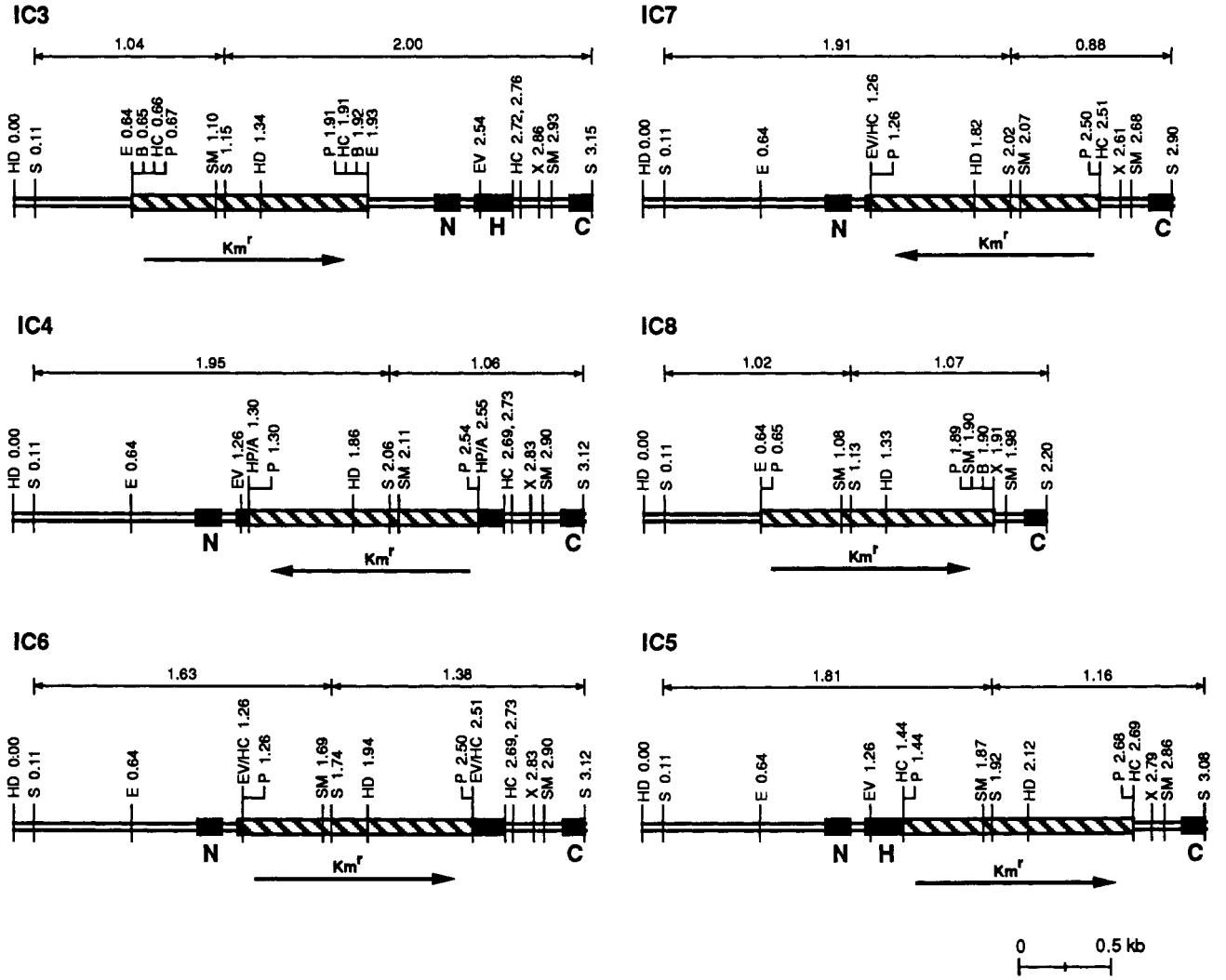

FIGURE 5: Restriction maps of mutant strains engineered with lesions in the *psbN–psbH–petC* region of the *Synechocystis* 6803 chromosome. The map numbers indicate the calculated distance in kilobases of predicted restriction sites from the *Hin*dIII site upstream of *psbH*. The distances were calculated using the known sequence of the cluster together with the published Km^r sequence (Taylor & Rose, 1988). Nucleotides 1–60 were only sequenced on one DNA strand and have not been reported (see Figure 1B). The sequence described by Mayes and Barber (1991) commences at nucleotide 61. The restriction sites shown are labeled as in Figure 1, with the following additions: A, *Acc*I; P, *Pst*I. Only the *Hpa*II site of Km^r ligation in IC4 is shown. Restriction sites that were ligated together during mutant construction are denoted with a /. The transcription direction of the Km^r is arrowed for each strain. The extent of *Ssp*I–*Ssp*I restriction fragments detected in the Southern analysis of Figure 6 is indicated above each map.

The results shown for IC7 (Figure 7A) are qualitatively similar to those obtained when IC4 or IC6 was plated. For these three strains, visible complementation with pSMH8 and also pSMH10 (not shown) was observed on PA plates, as is obvious from the appearance of the IC7 TI shown in Figure 7B, but not on PH or M plates. This visible complementation was due to the specific addition of the pSMH8 and pSMH10 plasmid inserts, since neither the addition of pUC18 nor the addition of just the buffer TE produced any discernible effect on any plating condition. Thus, it is evident that under the experimental conditions used, the *psbH*-less mutants have a markedly slower rate of photoautotrophic, but not photoheterotrophic or mixotrophic, growth compared to cells where *psbH* has been reintroduced.

Similar in situ complementation studies using IC8 and pSMH8 (not shown) further indicated that there were no obvious additional effects of deleting *psbN* alongside *psbH*. Thus, it is evident that a functional *psbN* gene is not essential for photoautotrophic growth under the conditions used. However, mutations affecting solely *psbN* expression are required to assess further the role of this gene.

Owing to the indistinguishable behavior in this screening of the three strains IC4, IC6, and IC7, where *psbH* has been specifically inactivated, only IC7 was selected for further phenotypic characterization. IC7 was chosen because, as a 3′ *psbH* deletion strain, it has no internal genetic potential for primary-site reversion to a *psbH*$^+$ strain. In liquid culture, under the conditions employed (see Materials and Methods), IC7 grew photoautotrophically at approximately 30% of the wild-type rate. This limited rate confirms the result from the growth on PA plates, that PS2 still assembles and functions in the absence of the PsbH protein. In further agreement with the in situ complementation studies, the difference between wild-type and IC7 growth rates was significantly reduced if glucose was added to the liquid culture medium.

Fluorescence. Variable fluorescence measurements can be used to probe the activity of PS2 centers and estimate their concentration per *Synechocystis* 6803 cell (Nixon & Diner, 1992; Nixon et al., 1992). As shown in Table I, the extent of variable chlorophyll fluorescence is lower in the IC7 mutant (F_v/F_m about 0.22) than the wild type (F_v/F_m about 0.33), and neither ratio is significantly affected by the presence or

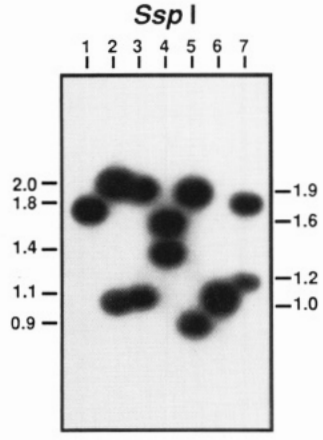

FIGURE 6: Verification of mutant strain genotypes by Southern analysis. Chromosomal DNA from wild-type and mutant strains was digested with *Ssp*I, fractionated on an 0.8% agarose gel, and transferred to nitrocellulose. The filter was hybridized at high-stringency with a DNA probe consisting of a 1:1 molar mixture of the plasmid pSMH10 insert containing *psbN* and *psbH* (see Figure 1B) and the isolated pUC4K kanamycin cartridge (Km^r). The resulting autoradiogram is shown after exposure for 4 days at −80 °C with intensifying screens. The lanes are (1) wild-type DNA, (2) IC3, (3) IC4, (4) IC6, (5) IC7, (6) IC8, and (7) IC5.

absence of DCMU, which blocks electron transfer between the plastoquinone acceptors of PS2, Q_A and Q_B. However, when the artificial electron donor hydroxylamine was added to DCMU-poisoned cells, the F_v/F_m value for IC7 increased to approximately 85% of that observed for similarly treated wild-type cells ($F_v/F_m = 0.31 \pm 0.01$ for IC7 and 0.36 ± 0.03 for the wild-type). Table I also shows that when electron transport between Q_A and Q_B is blocked by DCMU, the rate of fluorescence rise increased in the wild-type cells by a factor of about 3. In contrast, IC7 cells show a fast fluorescence rise in the absence of DCMU which is not signficantly increased by the addition of this electron-transport inhibitor.

Since the induction kinetics of IC7 resemble those of various herbicide-resistant mutants which are impaired in Q_A to Q_B electron transport [see Erickson et al. (1989)], we examined the kinetics of fluorescence decay following a single saturating flash (Figure 8). Single-flash fluorescence decay kinetics in the absence of DCMU provide information about how an electron generated by charge separation is shared on the acceptor side of PS2 between Q_A and Q_B. Previous work has shown that the decay has more than one phase. The initial fast decay phase, following flash excitation, is due to the reoxidation of Q_A^- by either Q_B or Q_B^- [depending on the preflash state of Q_B; see Astier et al. (1986) and Erickson et al. (1989)]. At longer times, the decay is more complex and can reflect the concentration of Q_A^- in equilibrium with Q_B or Q_B^- and/or the occupancy of the Q_B site (Astier et al., 1986; Etienne et al., 1990). Both decay curves shown in Figure 8A were fitted to two-exponential components as in Astier et al. (1986). The half-lifetime ($t_{1/2}$) of the fast component was determined to be 400 ± 32 μs in wild-type cells, in good agreement with comparable measurements from cyanobacteria and green algae (Astier et al., 1986; Erickson et al., 1989; Etienne et al., 1990), but a little slower than a determination from *Synechocystis* 6803 that employed slightly different conditions (Nixon & Diner, 1992). For IC7, the fast component $t_{1/2}$ was 800 ± 99 μs, indicating that Q_A^- oxidation by forward electron transport is slightly retarded compared to the wild type. However, the more dramatic difference in the decays concerns the slow component, which is much slower and larger in IC7 ($t_{1/2} = 42 \pm 14$ ms; overall contribution to

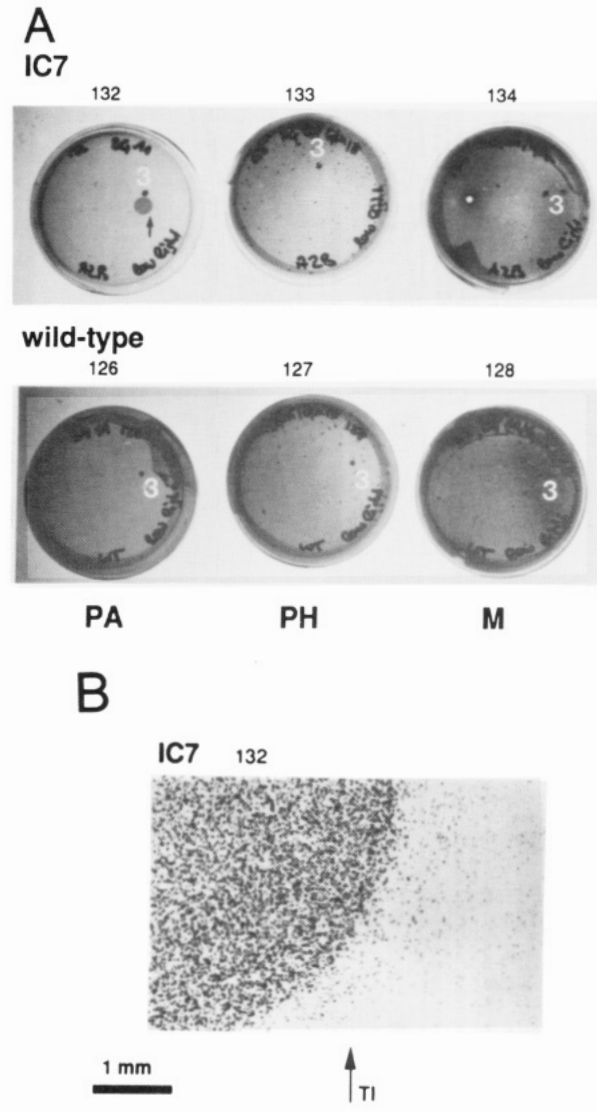

FIGURE 7: In situ complementation of *psbH* null mutant IC7 and the wild type under different growth conditions. Figure 7A shows typical results. Cyanobacterial agar overlays were poured on photoautotrophic growth plates (PA), photoheterotrophic growth plates (PH), or mixotrophic growth plates (M). These growth conditions are defined under Materials and Methods. The plates were spotted with 0.4–0.8 μg of unrestricted plasmid pSMH8 DNA (position 3) in 4–5 μL of TE buffer. Plasmid pSMH8 consists of the 4.2-kb *Synechocystis* 6803 *Hin*dIII–*Hin*dIII fragment containing *psbN*, *psbH*, *petC*, and *petA* (see Figure 1) subcloned into pUC18 (Yanisch-Perron et al., 1985). The appearances of the resulting plates after 7-days incubation at 32 °C under low light intensity illumination (5 μE m^{-2} s^{-1}) are shown. The site of the transformation interface enlarged in Figure 7B is arrowed on plate 132. Figure 7B shows the magnified transformation interface of plate 132. The mutant lawn is situated to the right of the arrow TI and the region where the wild-type gene was reintroduced is to the left.

decay curve = 42 ± 6%) than the wild type ($t_{1/2} = 2.5 \pm 0.3$ ms; contribution = 19 ± 3%). This difference suggests that in IC7, compared to the wild type, there is a decrease in the midpoint potential differences of the redox couples governing forward electron transport between the Q_A and Q_B sites and/or an increased population of Q_A^- that is not connected to the plastoquinone pool because of altered occupancy of the Q_B site. The latter possibility is illustrated in Figure 8B, where it can be seen that occupation of the Q_B site by DCMU in both wild-type and IC7 cells greatly increases the contribution of the slow component to the overall fluorescence decay.

Thermoluminescence Characteristics. Thermoluminescence was also used to investigate the redox properties of the

Table I: Fluorescence Characteristics of *Synechocystis* 6803 Wild-Type and IC7 Cells[a]

measured parameter	wild type		IC7	
	-DCMU	+DCMU	-DCMU	+DCMU
F_v/F_m	0.33 ± 0.02	0.36 ± 0.03	0.22 ± 0.04	0.23 ± 0.01
$t_{1/2}$ (ms)	1190	440	430	300

[a] Measurements were taken as described under Materials and Methods. F_m is the maximum fluorescence yield under continuous actinic illumination; F_0 is the initial fluorescence level seen when the actinic light is switched on; F_v is the variable fluorescence yield ($F_m - F_0$). The time taken to reach $^1/_2F_v$ is denoted $t_{1/2}$. Cells were resuspended at 30 μg of Chl *a* mL^{-1}; the DCMU concentration was 40 μM.

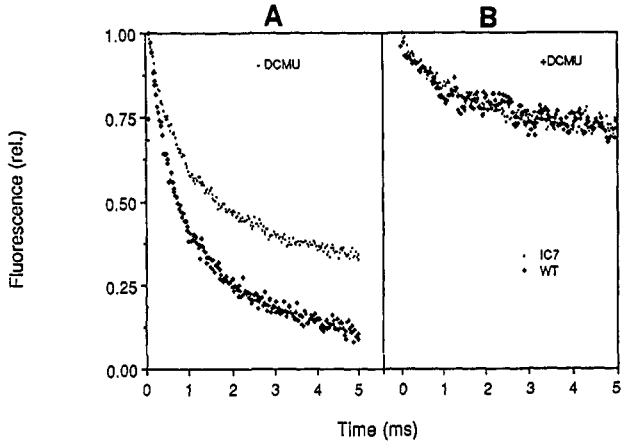

FIGURE 8: Effect of *psbH* gene inactivation on the decay of chlorophyll fluorescence from *Synechocystis* 6803. The decay was measured from wild-type and IC7 cells after giving an actinic flash of saturating light in order to totally reduce Q_A in the absence (A) and presence (B) of 40 μM DCMU. Curves were normalized to the maximum that occurred in 100 μs, which is time enough to exclude any disturbing flash artifacts. 40 μM DCMU blocks electron transport at the Q_B site to nearly 100%.

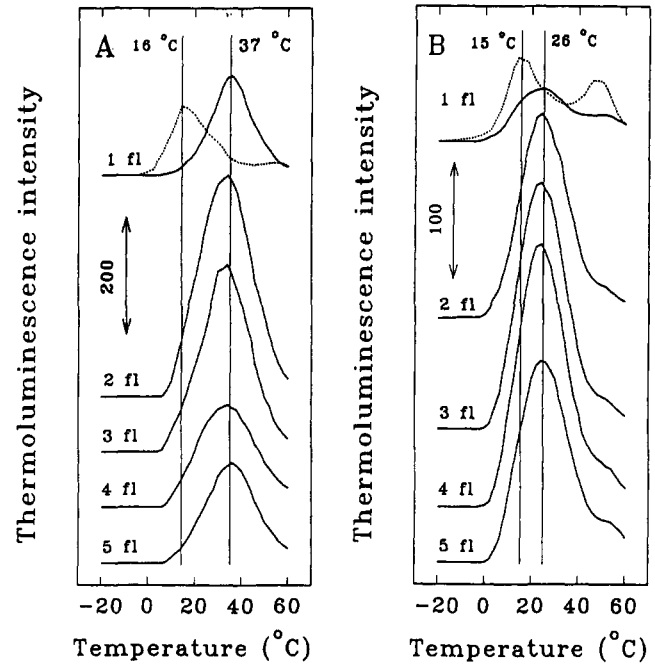

FIGURE 9: Effect of *psbH* gene inactivation on the flash-induced thermoluminescence of *Synechocystis* 6803. Thermoluminescence of wild-type (A) and IC7 cells (B) was measured at 50 μg of Chl *a* mL^{-1} after excitation with one to five flashes (solid curves) or after one flash in the presence of 40 μM DCMU (dashed curve).

acceptor side of PS2 in IC7 cells since it is a useful tool for studying charge stabilization and subsequent recombination in PS2 of higher plants or cyanobacteria. Radiative recombination of positive charges stored in the S_2 and S_3 oxidation states of the water-oxidizing complex with electrons stabilized on the reduced Q_A and Q_B acceptors of PS2 results in characteristic thermoluminescence emission [for recent reviews, see Sane and Rutherford (1986) and Vass and Inoue (1992)]. The thermoluminescence intensity reflects the amount of recombining charges, whereas the peak temperature is indicative of the energetic stabilization of the separated charge pair: the higher the peak temperature, the greater the stabilization (Vass et al., 1981). Illumination with one flash of plant material previously given a short dark pretreatment period induces a single thermoluminescence band, called the B-band, at around 35–40 °C, which arises from $S_2Q_B^-$ recombination (Rutherford et al., 1982; Demeter & Vass, 1984). If electron transfer between Q_A and Q_B is blocked by DCMU, the B-band is replaced by the so-called Q-band arising from $S_2Q_A^-$ recombination at around 10–15 °C (Rutherford et al., 1982; Demeter et al., 1982).

In wild-type *Synechocystis* 6803 cells, previously dark-adapted for 5 min, the B-band appears at around 37 °C and the Q-band at around 16 °C (Figure 9A). After illumination with two or more flashes, both the $S_2Q_B^-$ and the $S_3Q_B^-$ recombinations contribute to the B-thermoluminescence band whose intensity undergoes a characteristic period-four oscillation as a function of flash number. The oscillation of the B-band intensity reflects the redox cycling of the S-states (Sane & Rutherford, 1986; Vass & Inoue, 1992) and in the wild-type cells shows the first maximum after two flashes (Figure 10A), which is the usual observation for PS2 when given a short dark pretreatment.

In the IC7 mutant the B-band appears at around 25–27 °C (Figure 9B), which is about 10–12 °C lower than in the wild type. In contrast, the peak position of the Q-band, observed in the presence of DCMU, is about the same (15–16 °C) as in the wild-type cells (Figure 9B). The lower peak position of the B-band, together with the unchanged position of the Q-band, indicates a modification in the energetic stability of the electron on Q_B^- and thus a shift of the redox potential of the Q_B/Q_B^- redox couple to more negative values. Such a redox potential shift of Q_B can lower the equilibrium constant between Q_AQ_B and $Q_AQ_B^-$, leading to the accumulation of electrons on Q_A^- (Demeter et al., 1985). Indeed, a shoulder can be observed on the B-band of the mutant cells at the position of the Q-band, indicating a population of reduced Q_A without DCMU addition (Figure 9B, one flash). In the DCMU-treated mutant cells, a band at around 50 °C also appears. This is most likely the so-called C-band which originates from the recombination of Q_A^- with a donor side component which is not unambiguously identified yet (Sane & Rutherford, 1986; Vass & Inoue, 1992). The C-band can also be observed in the wild-type cells, but its appearance depends very much on the growing conditions.

For IC7, as for the wild type, the complete loss of the B-band emission following DCMU treatment indicates that 40 μM DCMU effectively blocks electron transport to the Q_B site. This is in agreement with the observation that neither IC7 nor the wild type will grow on PA plates supplemented with 10 μM DCMU.

The intensity of the B-band is rather low in the IC7 cells after the first flash and reaches only about 20% of that in the wild-type cells. After the second and third flashes, the B-band intensity increases substantially (Figure 9B) but afterward shows a very dampened oscillation (Figure 10A). In order to compare the oscillatory patterns of IC7 and wild-type cells, which have different intensities in the steady-state level, the

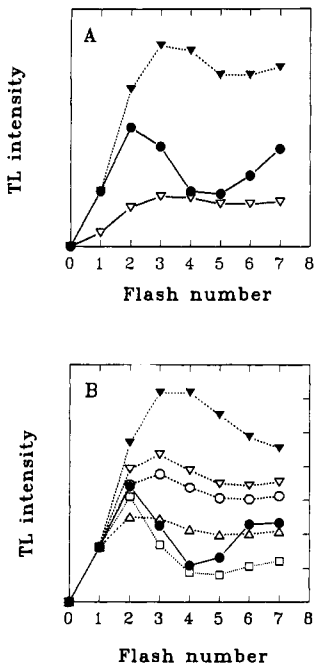

FIGURE 10: Effect of *psbH* gene inactivation on the flash-induced oscillation of the B thermoluminescence band of *Synechocystis* 6803. (A) Experimental results: Thermoluminescence of wild-type (closed circles) and IC7 (open triangles) cells was measured after excitation with various numbers of flashes at 5 °C. The oscillation of the B-band intensity in the mutant cells is also shown after normalization of the first flash intensity to the same value as obtained in the wild-type cells (closed triangles). (B) Model calculations: The oscillation of the B-band was simulated by assuming S_0:S_1:S_2:S_3 = 0.25:0.75:0:0; Q_B:Q_B^- = 0.5:0.5 initial distribution of states. For the oscillation of the wild-type cells, 17% miss and 3% double-hit parameters were used (closed circles). To simulate the oscillation of IC7 cells, either a 77% miss was assumed at the $S_0 \rightarrow S_1$ (open squares), $S_1 \rightarrow S_2$ (inverted open triangles), $S_2 \rightarrow S_3$ (open triangles), or $S_3 \rightarrow S_0$ transition (open circles), or a 52% miss at all transitions (inverted closed triangles) plus a Q_B:Q_B^- = 0.3:0.7 initial distribution. Each simulated oscillatory pattern is shown after normalization for the intensity obtained after the first flash.

B-band intensities were normalized to the same value after the first flash (Figure 10A, dashed curve). This representation clearly shows the unusually large increase of thermoluminescence intensity from IC7 cells after the second flash, as well as the almost complete lack of oscillation after three or more flashes.

A simulation of the B-band oscillation was performed to interpret the modified oscillation in IC7 cells on the basis of the model presented in Demeter and Vass (1984) with the inclusion of about 50% thermoluminescence yield of the $S_2Q_B^-$ recombination relative to that of the $S_3Q_B^-$ recombination (Sane & Rutherford, 1986). This simulation shows that a specific inhibition of any of the S-state transitions alone would give a modification of the B-band oscillation (Figure 10B) which is largely different from the experimental result (Figure 10A). The modified oscillation pattern in the mutant cells can be satisfactorily explained by the combination of two assumptions: (i) increased probability of misses at all S-state transitions (or at the S_1 to S_2 or S_3 to S_0 transition, not shown) to interpret the dampening of the oscillation; (ii) a largely reduced state of the B-band intensity after the second flash. It is of note that this latter assumption could be replaced with a modified distribution of S-states in the dark (about 50% S_0 and 50% S_1 instead of the usual 25% S_0 and 75% S_1, not shown).

Oxygen Evolution. To obtain further information about the functioning of PS2 in the absence of the *psbH* gene product, both steady-state and flash-induced oxygen evolution was measured. The steady-state rate of oxygen evolution is largely dependent on the electron acceptor used (Table II). In the absence of artificial electron acceptors, the oxygen rate in the mutant cells was nearly as high as in the wild type. Addition of 1 mM dimethyl-*p*-benzoquinone (DMQ), or 1 mM DMQ plus 1 mM potassium ferricyanide (FeCy), increased the oxygen rate in the wild type by 50–70%. In contrast, with mutant cells, these acceptors decreased the oxygen rate to almost half of that measured without acceptors. In the presence of 1 mM dichlorobenzoquinone (DCBQ), the oxygen rate is increased by 80% and 30% in the wild-type and mutant cells, respectively. Since DMQ accepts electrons from the Q_B site, whereas DCBQ acts at the Q_A site (Graan & Ort, 1986), these results point to the modification of the Q_B site, in agreement with the thermoluminescence data.

Table II: Steady-State Rates of Oxygen Evolution from *Synechocystis* 6803 Wild-Type and IC7 Cells[a]

acceptor	wild type	IC7
no additions	100	95 (95)
1 mM DMQ	150	50 (33)
1 mM DMQ + 1 mM FeCy	172	61 (35)
1 mM DCBQ	182	130 (71)

[a] The rates are shown in arbitrary units using the 100 value for the rate from wild-type cells without added acceptors except for CO_2 dissolved in the medium. Values in parentheses are the percent values of the oxygen evolution rates of IC7 cells relative to that of the wild-type in the presence of the same acceptor. The data are based on at least three to four different experiments. The variability of the measurements was about 3–5% within the same culture and 10–15% between different cultures.

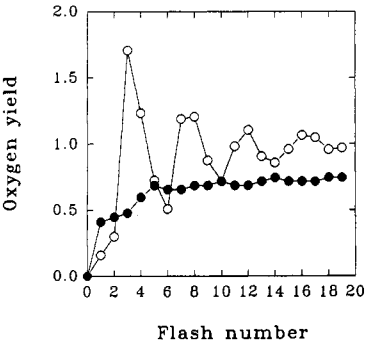

FIGURE 11: Effect of *psbH* gene inactivation on the flash-induced oscillation of oxygen evolution in *Synechocystis* 6803. Oxygen yield in a sequence of flashes was measured from wild type (open circles) and IC7 (closed circles) at 50 μg of Chl *a* mL^{-1}. The frequency of the exciting flashes was 1 Hz.

The flash yield of oxygen evolution in the wild-type cells has the same pattern as reported earlier for *Synechocystis* 6803 (Cao et al., 1991; Vass et al., 1992), including the unusual electrochemical signals on the first and second flashes (Figure 11). The flash pattern of oxygen evolution from the mutant showed an increased signal on the first two flashes, accompanied by a large degree of dampening in the whole sequence (Figure 11). The steady-state yield of flash-induced oxygen evolution reached a level which is comparable to that in the wild-type cells. The increased dampening of oxygen evolution from IC7 indicates that this mutant has a limited capacity for S-state turnovers, in agreement with the thermoluminescence results. However, oxygen evolution measurements and model calculations do not help to clarify whether the increased misses occur at a particular, or at each, S-state transition since oxygen release during the final S_3 to S_0 transition is also influenced by misses that occur earlier.

DISCUSSION

In this work, we have further characterized the gene cluster containing *psbH* in *Synechocystis* 6803. We then use this knowledge to examine the phenotypic consequences of specifically inactivating *psbH* in vivo.

A restriction map of about 25.1 kb of the *Synechocystis* 6803 chromosome containing *psbN*, *psbH*, *petC*, and *petA* has been generated. Southern hybridization (not presented) has directly established that neither *psbB* nor *psbO* resides in this region. Furthermore, the map has been compared with all the available restriction data from other cloned *Synechocystis* 6803 genes, but no similarities were recognized. We could deduce that the *psbH* cluster is not closely linked to other characterized genes involved in photosynthesis (PS2, photosystem 1, and the ATP synthase), apart from *psbD2* and *psbEFLJ*, where insufficient restriction data have been reported [the available data for these two loci are summarized in Nixon et al. (1992)].

Although we report that *petC* and *petA* exist as single copies in *Synechocystis* 6803, it should be noted that our low-stringency Southern analysis would not have detected genes for equivalent components of a bacterial/mitochondrial-type cytochrome bc_1 complex. While no such complex has been characterized in cyanobacteria, the recent characterization of an antimycin A-sensitive NADPH or plastoquinol-9/cytochrome *c* oxidoreductase activity in the plasma membranes of four different cyanobacteria (Kraushaar et al., 1990) means this possibility cannot be excluded.

Linkage of psbN and psbH to pet Genes in Cyanobacteria and Plant Chloroplasts. Much evidence has accumulated that chloroplasts evolved from the endosymbiosis of an ancestral cyanobacterium into a eukaryotic cell [see Gray (1989)]. Indeed, many cotranscribed gene clusters appear to have been conserved between cyanobacterial and chloroplast genomes, including the *psbD–psbC* (Golden & Stearns, 1988), *psbE–psbF–psbL–psbJ* (Nyhus & Pakrasi, 1989), *ndhC–ndhK1* (*psbG1*)*–ndhJ* (Steinmüller et al., 1989), *psaA–psaB* (Cantrell & Bryant, 1987) and *atpB–atpE* (Cozens & Walker, 1987) clusters. Thus, the linkage of *psbN–psbH* to genes encoding different subunits of the cytochrome b_6–*f* complex in the genomes of *Synechocystis* 6803 and plant chloroplasts represents a very interesting situation which may imply a functional reason for these gene associations. It was surprising, therefore, that our results suggest that *psbH* and *petCA* are transcribed as separate mono- and dicistronic mRNAs in *Synechocystis* 6803. Processing of a primary transcript covering *psbH*, *petC*, and *petA* in a manner similar to that seen in either the plant chloroplast *psbB* operon [see Westhoff and Herrmann (1988) and Westhoff et al. (1991)] or the *puf* operon of purple photosynthetic bacteria (Belasco et al., 1985) seems unlikely for the following reasons: (i) Northern analysis did not detect a transcript encompassing *psbH*, *petC*, and *petA*. (ii) The absence of a series of 5′ *petCA* transcript termini in the primer extension analysis suggests that the detected end points represent initiation points, especially since the region upstream of this site, the putative *petCA* promoter (see below), has some homology with *E. coli* σ^{70} promoter consensus sequence. (iii) The insertion of Km^r immediately downstream of *psbH* in control strain IC5 had no obvious effect on the growth rate in the range of conditions monitored in the in situ complementation studies. (iv) *petC* and *petA* are cotranscribed as a dicistronic transcript in two other cyanobacteria, *Nostoc* PCC 7906 (Kallas et al., 1988) and *Synechococcus* sp. PCC 7002 (Widger, 1991).

Our data therefore suggest that the clustering of *psbN* and *psbH* with different *pet* genes across species either is due to a reason other than the coordination of gene expression via cotranscription or is fortuitous. However, it remains possible that cotranscription occurs in growth conditions not investigated in our experiments. The possibility that, in the past, *psbH* was cotranscribed with *petCA* and that separate transcription developed more recently in evolution cannot be totally discounted either. In any event, the conserved organization of *psbN* and *psbH* in *Synechocystis* 6803 and in the chloroplast suggests this is an ancestral gene association.

Synechocystis 6803 Promoters. The identification of candidate promoter regions in *Synechocystis* 6803 is important because although this organism has been used for a number of mutagenesis studies [reviewed by Nixon et al. (1992) and Pakrasi and Vermaas (1992)], little is known about the DNA sequences regulating transcription. Following from the above discussion regarding transcription, we conclude that the 5′-transcript end points mapped by primer extension represent transcription initiation points. Thus, we have identified two putative promoter regions upstream of *psbH* and one upstream of *petC*. The region upstream of *psbH* P1 shows strong similarity to an *E. coli* σ^{70} consensus promoter sequence. That upstream of *psbH* P2 is different as it only has an element with clear similarity to the σ^{70} "–10" region. The region preceding the *petC* initiation point also bears some resemblance to the σ^{70} consensus sequence.

While the transcription initiation point has only been determined for one other *Synechocystis* 6803 gene (Ravnikar et al., 1990), more sites have been mapped in other cyanobacterial species. Interestingly, a number are preceded by both σ^{70} "–10"- and "–35"-like elements and others just by the "–10" element (Zhang, 1992). As elements similar to the σ^{70} consensus sequence function as promoter elements in *Bacillus subtilis* (Helmann & Chamberlin, 1988) and in chloroplasts (Hanley-Bowdoin & Chua, 1987), there is reason to suppose they may also be functional in cyanobacteria.

The observation of two potential promoters for *psbH* is not without precedent. Dual promoters have also previously been described upstream of other cyanobacterial genes including various *cpc* operons, e.g., *Synechocystis* sp. PCC 6701 (Anderson & Grossman, 1990), the *glnA*, *psbB*, and *atpB* genes of *Anabaena* sp. PCC 7120 (Tumer et al., 1983; Lang & Haselkorn, 1989; Curtis, 1987), and also *psbAII* of *Synechococcus* sp. PCC 7942 (Bustos et al., 1990), and are also common in *E. coli* [see Collado-Vides et al. (1991)]. It is tempting to speculate that the two putative *psbH* promoters respond to different regulatory signals as, for example, is the case with the *Anabaena* sp. PCC 7120 *glnA* gene (Tumer et al., 1983) although specific factors affecting *psbH* transcription have yet to be identified.

Consequences of Inactivating psbH in Synechocystis 6803. We were able to segregate *psbH* null mutants under photoheterotrophic conditions which grew photoautotrophically, photoheterotrophically, and mixotrophically in the in situ complementation assay. In contrast, it has not proved possible to inactivate *Synechocystis* 6803 genes encoding components essential for PS1 activity using similar segregation conditions (Smart et al., 1991). Furthermore, our results show that the in situ complementation assay is a simple, rapid screening technique for not only confirming a mutant genotype but also delivering a preliminary assessment of the consequences of target gene inactivation in *Synechocystis* 6803. We now routinely use this procedure for initial screening of all the targeted mutants generated in the laboratory. In this work,

the in situ complementation assay provided the first indication that inactivation of *psbH* primarily affects PS2 activity, since only the photoautotrophic growth capacity appeared to be noticeably reduced in the screening procedure. This reduction was subsequently confirmed for IC7 through measuring growth rates in liquid culture.

Biophysical Characterization of Mutant IC7. The observation that IC7 and the other *psbH* null mutants retain some photoautotrophic growth capability clearly demonstrates that the PsbH protein is not essential for PS2 activity in *Synechocystis* 6803. However, several noninvasive biophysical techniques have confirmed a functional role for the protein in PS2.

The variable fluorescence yield in the presence of hydroxylamine and DCMU can be used to estimate the level of PS2 in *Synechocystis* 6803 mutants (Nixon & Diner, 1992). Since the F_v/F_m value for IC7 with these additions was about 85% that of the wild type, this suggests that, to a first approximation, the number of assembled PS2 centers per cell is not drastically altered by *psbH* inactivation. Such a conclusion is supported by the relatively high rate of steady-state oxygen evolution from IC7 when DCBQ is added. Thus, unlike the general situation found when genes encoding other intrinsic subunits of PS2 are inactivated in *Synechocystis* 6803 [reviewed by Nixon et al. (1992)] substantial levels of PS2 still seem to assemble in the absence of a functional *psbH* gene.

IC7 cells have several alterations of PS2 electron transfer relative to that of the wild type. In part, these alterations indicate a modification of the Q_B binding site, as suggested by the following: (i) Variable fluorescence in the absence of DCMU rises faster in the mutant than in the wild-type cells, indicating a slowing down in Q_A to Q_B electron transfer. (ii) A decrease in the kinetics of Q_A^- oxidation in the mutant is detected by chlorophyll fluorescence decay after a single saturation flash, with, in particular, a notable increase in $t_{1/2}$ and the contribution of the slow decay component. (iii) The peak position of the B ($S_2Q_B^-$ recombination) but not of the Q ($S_2Q_A^-$ recombination) thermoluminescence band is shifted to lower temperatures by about 10–12 °C. This situation resembles that observed in herbicide-resistant mutants which have modified Q_B sites (Demeter et al., 1985) and might indicate altered Q_B binding-site properties and/or a decrease in the redox potential of the Q_B/Q_B^- redox couple in IC7; both these possibilities are consistent with the single-flash fluorescence decay data. (iv) The unusually high ratio of B-band intensities after two flashes versus one (about three to four) shows the small population of the S_1Q_B state (from which $S_2Q_B^-$ is formed by one flash) in mutant cells dark-adapted for short times. This probably originates from the shifting of the dark distributions of Q_B to Q_B^- from about 50:50% (usually observed in PS2 after short dark-preadaptation) toward about 30:70%, indicating an increasingly reduced state of Q_B in the mutant cells. However, the modification of the dark distribution of S-states (from an S_0:S_1 ratio = 25:75% to about 50:50%) cannot be completely excluded at present either. (v) The rate of steady-state oxygen evolution is largely decreased in IC7 relative to the wild type when measured in the presence of DMQ, but not in the presence of DCBQ. This difference is likely to arise when DMQ accepts electrons from the Q_B site and DCBQ from the Q_A site, thus indicating a modification of the Q_B binding site.

The very large dampening of flash-induced oxygen evolution and of the B-band oscillation shows a high probability of misses in PS2 devoid of the PsbH protein. Even though the thermoluminescence oscillation data do not provide unambiguous proof, it is likely that the increased misses are not limited to a particular S-state transition but affect the function of PS2 uniformly after each flash. Large dampening of oxygen evolution can also be observed in herbicide-resistant organisms (Vermaas et al., 1984) in which the Q_B binding region is modified due to point mutations in the D1 reaction center protein and therefore the increased probability of misses might arise as a consequence of the modified Q_B binding region in IC7. However, a larger scale structural modification of PS2 which directly affects the water-oxidizing reactions in the absence of the PsbH protein cannot be excluded here. A slowing down of water-oxidizing activity in IC7 could also provide an explanation for the smaller variable fluorescence detected in the absence of hydroxylamine and the decreased steady-state level of the B-band intensity and could contribute to the reduction in the maximum rate of oxygen evolution rate recorded in the presence of DMQ. In summary, it is possible that the absence of the PsbH protein exerts an influence on the donor side of PS2, in addition to the obvious acceptor side effect.

The *psbH* gene product of the chloroplast genome has been identified as the 9-kDa phosphoprotein of the PS2 complex (Bennett, 1977). Many of the characteristic modifications of PS2 electron transport in the *psbH*-less mutant IC7 resemble those observed, to a lesser extent, after the phosphorylation of the 9-kDa protein. These include the decrease of the oxygen evolution rate (Hodges et al., 1985), a smaller variable fluorescence with no additions (Hodges et al., 1987), the energetic destabilization of Q_B^- which leads to the decrease of the equilibrium constant between $Q_A^-Q_B$ and $Q_AQ_B^-$, and a change in the flash pattern of oxygen evolution (Packham et al., 1988). The physiological role of the 9-kDa phosphoprotein is not yet clarified. Among other proposals, it has been suggested to be involved in the regulation of electron transfer between Q_A and Q_B (Packham, 1988). The surprisingly similar consequences of the phosphorylation and of the absence of the PsbH protein raise the possibility that its presumed regulatory role is achieved via conformational changes that influence the structure of the Q_B binding niche on the D1 protein. Such a role would assume the location of the 9-kDa protein in the close proximity of the D1 protein where it could directly affect the Q_B site. We have not, however, found sufficient sequence homology between the *Synechocystis* 6803 PsbH protein and the reaction center H-subunit of purple photosynthetic bacteria to suggest these proteins evolved directly from a common ancestral protein as proposed by Packham (1988).

ACKNOWLEDGMENTS

We especially thank Dr. Z.-H. Zhang and A. Jarhaus for assistance with experiments and also Dr. S. J. Self for help in constructing strain IC8. Thanks also to Dr. J. G. K. Williams for providing the *Synechocystis* 6803 strain used in these studies and to Dr. D. A. Bryant, Dr. P. J. Nixon, Dr. W. G. F. Whitfield, and members of the AFRC Photosynthesis Research Group for helpful discussion.

REFERENCES

Abdel-Mawgood, A. L., & Dilley, R. A. (1990) *Plant Mol. Biol. 14*, 445–446.

Allen, J. F., Bennett, J., Steinback, K. E., & Arntzen, C. J. (1981) *Nature 291*, 25–29.

Anderson, L. K., & Grossman, A. R. (1990) *J. Bacteriol. 172*, 1289–1296.

Anderson, S. L., & McIntosh, L. (1991) *J. Bacteriol. 173*, 2761–2767.
Andersson, B., & Styring, S. (1991) *Curr. Top. Bioenerg. 16*, 1–81.
Astier, C., Elmorjani, K., Meyer, I., Joset, F., & Herdman, M. (1984) *J. Bacteriol. 158*, 659–664.
Astier, C., Meyer, I., Vernotte, C., & Etienne, A.-L. (1986) *FEBS Lett. 207*, 234–238.
Ausubel, F. M., Brent, R., Kingston, R. E., Moore, D. D., Seidman, J. G., Smith, J. A., & Struhl, K. (1987) *Current Protocols In Molecular Biology*, Vol. 1, John Wiley & Sons, New York.
Belasco, J. G., Beatty, J. T., Adams, C. W., von Gabain, A., & Cohen, S. N. (1985) *Cell 40*, 171–181.
Bennett, J. (1977) *Nature 269*, 344–346.
Bustos, S. A., Schaefer, M. R., & Golden, S. S. (1990) *J. Bacteriol. 172*, 1998–2004.
Cantrell, A., & Bryant, D. A. (1987) *Plant Mol. Biol. 9*, 453–468.
Cao, J., Vermaas, W. F. J., & Govindjee (1991) *Biochim. Biophys. Acta 1059*, 171–180.
Collado-Vides, J., Magasanik, B., & Gralla, J. D. (1991) *Microbiol. Rev. 55*, 371–394.
Cozens, A. L., & Walker, J. E. (1987) *J. Mol. Biol. 194*, 359–383.
Curtis, S. E. (1987) *J. Bacteriol. 169*, 80–86.
Demeter, S., & Vass, I. (1984) *Biochim. Biophys. Acta 764*, 24–32.
Demeter, S., Droppa, M., Vass, I., & Horvath, G. (1982) *Photobiochem. Photobiophys. 4*, 163–168.
Demeter, S., Vass, I., Hideg, É., & Sallai, A. (1985) *Biochim. Biophys. Acta 806*, 16–24.
Dzelzkalns, V. A., & Bogorad, L. (1988) *EMBO J. 7*, 333–338.
Erickson, J. M., Pfister, K., Rahire, M., Togasaki, R., Mets, L., & Rochaix, J.-D. (1989) *Plant Cell 1*, 361–371.
Etienne, A.-L., Ducret, J.-M., Ajlani, G., & Vernotte, C. (1990) *Biochim. Biophys. Acta 1015*, 435–440.
Golden, S. S., & Stearns, G. W. (1988) *Gene 67*, 85–96.
Graan, T., & Ort, D. R. (1986) *Biochim. Biophys. Acta 852*, 320–330.
Gray, M. W. (1989) *Trends Genet. 5*, 294–299.
Hanley-Bowdoin, L., & Chua, N.-H. (1987) *Trends Biochem. Sci. 12*, 67–70.
Harley, C. B., & Reynolds, R. P. (1987) *Nucleic Acids Res. 15*, 2343–2359.
Helmann, J. D., & Chamberlin, M. J. (1988) *Annu. Rev. Biochem. 57*, 839–872.
Hird, S. M., Dyer, T. A., & Gray, J. C. (1986) *FEBS Lett. 209*, 181–186.
Hodges, M., Packham, N. K., & Barber, J. (1985) *FEBS Lett. 181*, 83–87.
Hodges, M., Boussac, A., & Briantais, J.-M. (1987) *Biochim. Biophys. Acta 894*, 138–145.
Ikeuchi, M., Koike, H., & Inoue, Y. (1989) *FEBS Lett. 253*, 178–182.
Kallas, T., Spiller, S., & Malkin, R. (1988) *Proc. Natl. Acad. Sci. U.S.A. 85*, 5794–5798.
Kohchi, T., Yoshida, T., Komano, T., & Ohyama, K. (1988) *EMBO J. 7*, 885–891.
Knaff, D. B. (1991) *Trends Biochem. Sci. 16*, 82–83.
Kraushaar, H., Hager, S., Wastyn, M., & Pescheck, G. A. (1990) *FEBS Lett. 273*, 227–231.
Kuhn, M., Thiel, A., & Boger, P. (1988) *Z. Naturforsch. 43C*, 413–417.
LaBarre, J., Chauvat, F., & Thuriaux, P. (1989) *J. Bacteriol. 171*, 3449–3457.
Lang, J. D., & Haselkorn, R. (1989) *Plant Mol. Biol. 13*, 441–456.
Maniatis, T., Fritsch, E. F., & Sambrook, J. (1982) *Molecular Cloning, A Laboratory Manual*, Cold Spring Harbor Laboratory, Cold Spring Harbor, NY.
Mayes, S. R. (1992) Ph.D. Thesis, University of London.
Mayes, S. R., & Barber, J. (1990) *Nucleic Acids Res. 18*, 194.
Mayes, S. R., & Barber, J. (1991) *Plant Mol. Biol. 17*, 289–293.
Mayes, S. R., Cook, K. M., & Barber, J. (1990) in *Current Research in Photosynthesis* (Baltscheffsky, M., Ed.) Vol. III, pp 617–620, Kluwer, Dordrecht, The Netherlands.
Mayes, S. R., Cook, K. M., Self, S. J., Zhang, Z.-H., & Barber, J. (1991) *Biochim. Biophys. Acta 1060*, 1–12.
Nixon, P. J., & Diner, B. A. (1992) *Biochemistry 31*, 942–948.
Nixon, P. J., Rögner, M., & Diner, B. A. (1991) *Plant Cell 3*, 383–395.
Nixon, P. J., Chisholm, D. A., & Diner, B. A. (1992) in *Plant Protein Engineering Shrewry*, P., & Gutteridge, S., Eds.) pp 93–141, Cambridge University Press, Cambridge, U.K.
Nyhus, K. J., & Pakrasi, H. B. (1989) in *Techniques and New Developments in Photosynthesis Research* (Barber, J., & Malkin, R., Eds.) pp 469–472, Plenum Press, New York.
Packham, N. K. (1988) *FEBS Lett. 231*, 284–290.
Packham, N. K., Hodges, M., Etienne, A.-L., & Briantais, J. M. (1988) *Photosynth. Res. 15*, 221–232.
Pakrasi, H. B., & Vermaas, W. F. J. (1992) in *The Photosystems: Structure, Function and Molecular Biology, Topics in Photosynthesis* (Barber, J., Ed.) Vol. 11, pp 231–257, Elsevier, Amsterdam.
Philbrick, J. B., Diner, B. A., & Zilinskas, B. A. (1991) *J. Biol. Chem. 266*, 13370–13377.
Ravnikar, P., Sithole, I., Debus, R., Babcock, G., & McIntosh, L. (1990) in *Current Research in Photosynthesis* (Baltscheffsky, M., Ed.) Vol. III, pp 499–507, Kluwer, Dordrecht, The Netherlands.
Rippka, R. (1972) *Arch. Mikrobiol. 87*, 93–98.
Rutherford, A. W., Crofts, A. R., & Inoue, Y. (1982) *Biochim. Biophys. Acta 682*, 457–465.
Sane, P. V., & Rutherford, A. W. (1986) in *Light Emission by Plants and Bacteria* (Govindjee, Amesz, J., & Fork, D. C., Eds.) pp 329–361, Academic Press, New York.
Smart, L. B., Anderson, S. L., & McIntosh, L. (1991) *EMBO J. 10*, 3289–3296.
Smith, A. J. (1982) in *The Biology of the Cyanobacteria* (Carr, N. G., & Whitton, B. A., Eds.) pp 47–86, Blackwell Scientific Publications, Oxford, U.K.
Steinmüller, K., Ley, A. C., Steinmetz, A. A., Sayre, R. T., & Bogorad, L. (1989) *Mol. Gen. Genet. 216*, 60–69.
Taylor, L. A., & Rose, R. E. (1988) *Nucleic Acids Res. 16*, 358.
Tumer, N. E., Robinson, S. J., & Haselkorn, R. (1983) *Nature 306*, 337–342.
Vass, I., & Inoue, Y. (1992) *Top. Photosynth. 11*, 259–294.
Vass, I., Horváth, G., Herczeg, T., & Demeter, S. (1981) *Biochim. Biophys. Acta 634*, 140–152.
Vass, I., Deák, Zs., & Hideg, É. (1990) *Biochim. Biophys. Acta 1017*, 63–69.
Vass, I., Cook, K. M., Deák, Zs., Mayes, S. R., & Barber, J. (1992) *Biochim. Biophys. Acta 1102*, 195–201.
Vermaas, W. F. J., Dohnt, G., & Renger, G. (1984) *Biochim. Biophys. Acta 806*, 16–24.
Vieira, J., & Messing, J. (1982) *Gene 19*, 259–268.
Westhoff, P., & Hermann, R. G. (1988) *Eur. J. Biochem. 171*, 551–564.
Westhoff, P., Farchaus, J. W., & Hermann, R. G. (1986) *Curr. Genet. 11*, 165–169.
Westhoff, P., Offermann-Steinhard, K., Höfer, M., Eskins, K., Oswald, A., & Streubel, M. (1991) *Planta 184*, 377–388.
Widger, W. R. (1991) *Photosynth. Res. 30*, 71–84.
Williams, J. G. K. (1988) *Methods Enzymol. 167*, 766–778.
Yanishch-Perron, C., Vieira, J., & Messing, J. (1985) *Gene 33*, 103–119.
Zhang, Z.-H. (1992) Ph.D. Thesis, University of London.